

the host galaxy to be a giant elliptical in agreement with previous studies but with probably a faint stellar disk. A similar feature was also found in the galaxy hosting the BL Lac PKS 0548–32 and may be not uncommon in early-type galaxies (see e.g. Scorza 1992). Its relation with the active nucleus (e.g. by accretion events) needs, however, a complete study for a larger sample of objects.

The optical jet is markedly knotty and resembles that of M 87 although it is more than a factor of 2 intrinsically brighter in the R band (cf. Biretta *et al.* 1991). Also the projected length of the jet (10 kpc) is much larger than that (~ 2 kpc) observed in M 87. The presence of the secondary peak (B) was suggested by the FOC image obtained with HST before the introduction of COSTAR and is well detected here. The decreasing optical intensity along the jet follows a behaviour very similar to that observed at 2 cm by Keel (1986).

Although the feature (C) is resolved, it remains unclear whether it is associated with the jet in some way or whether it is just a projected object. The lack of radio emission and of optical polarization favours the hypothesis that it is a projected faint galaxy. The centre of the ‘red tip’ is however very closely aligned with the bright knot and the centre of the galaxy.

Acknowledgement

I wish to thank G. Fasano for his kind assistance in the use of the AIAP package.

References

- Biretta, J.A., Stern, C.P., and Harris, D.E. 1991, *AJ*, **101**, 1632.
 Boisson, C., Cayatte, V., Sol, H. 1989, *A&A*, **211**, 275.
 Cayatte, V., and Sol, H. 1987, *A&A*, **171**, 25.

- Danziger, I.J., Fosbury, R.A.E., Goss, W.M., and Ekers, R. D. 1979, *MNRAS*, **188**, 415.
 Danziger, I.J., Shaver, P.A., Moorwood, A.F. M., Fosbury, R.A.E., Goss, W.M., and Ekers, R.D. 1985, *The Messenger*, **39**, 20.
 Fichtel, C. E., et al. 1994, *ApJS*, in press.
 Keel, W. C. 1986, *ApJ*, **302**, 296.
 Macchetto, F., et al. 1991, *ApJ*, **369**, L55.
 Pian, E., Falomo, R., Ghisellini, G., Maraschi, L., Sambruna, R.M., Scarpa, R. & Treves, A. 1994, *ApJ*, submitted.
 Reduzzi, L. *et al.*, 1994, *The Messenger*, **75**, 28.
 Scarpa, R., Falomo, R., & Pian, E. 1994, *PASP*, submitted.
 Scorza, C., 1992, ESO/EIPC Workshop, *Structure, Dynamics and Chemical Evolution of Elliptical Galaxies*, p. 115, Ed. I.J. Danziger *et al.*
 Sparks, W. B., Miley, G. K., and Macchetto, F. 1990, *ApJ*, **361**, L41.
 Ulrich, M. H. 1981, *A&A*, **103**, L1.

Molecular Hydrogen Observations Towards Herbig-Haro Objects

R. GREDEL, ESO-La Silla

1. Introduction

The small optical line emission nebulae known as Herbig-Haro (HH) objects have received considerable attention in recent years. This is because HH objects are associated with young stellar objects, and their study may give insight into the processes that occur during star formation. It is believed that during the formation of a low-mass star a collimated jet of material is produced that emerges with supersonic speeds. The formation of jets may help to remove angular momentum from the forming stars. In the interaction regions of the jets with the ambient interstellar medium, bow shocks are created where the bulk energy of the outflowing material is converted into thermal energy. Temperatures in the shocks are raised to 2000–3000 K.

In recent years, it became evident that HH objects are also prominent emitters of molecular hydrogen lines in the near-infrared. To our delight, the near-infrared emission offers new possibilities to study the processes that occur in the shocked gas. The ground state of H₂ has a multitude of vibration-rotation levels with excitation energies ranging from less than 1000 K to several 10,000 K. The lowest levels, with vibrational quantum number

$v \leq 3$, can be collisionally excited in the shock-heated gas. This case is referred to as thermal excitation. Levels above $v > 3$ are too high in energy and are not excited.

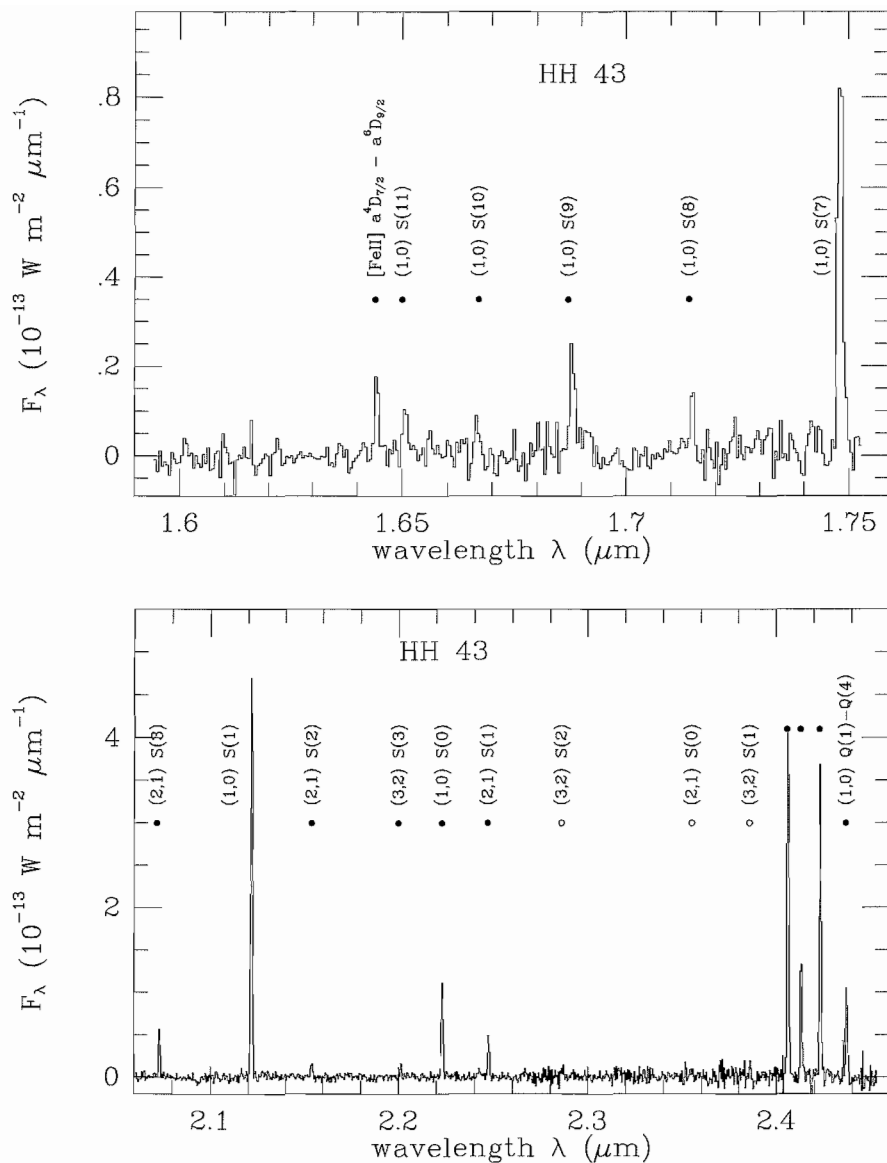
Two alternative, non-thermal, excitation mechanisms have also been discussed in connection with HH flows. In many cases the shocks are fast enough to produce ultraviolet and X-ray photons. The radiation might fluorescently excite the electronic states of H₂, or lead to excitation of the electronic states via impact by the secondary electrons produced by the X-rays. The decay of the electronic states competes with the collisions to populate the vibrational levels in the ground state, and, in particular, it populates levels in $v > 3$. If the shock speeds become too high, the shocks are dissociative and H₂ is destroyed. Nevertheless, H₂ emission can still occur, because H₂ eventually re-forms in the post-shock region where the gas is cooling. Part of the energy that is released when two H atoms combine to form H₂ is converted into excitations of the vibrational levels, which also include $v > 3$.

It has been suggested that each of the non-thermal excitation scenarios described here is strong enough to lead to observable effects. Schwartz *et al.*

(1987) have performed calculations for the specific case of HH 43. The authors considered excitations by ultraviolet Ly α photons and predicted the resulting near-infrared emission spectrum. They also obtained a low-resolution CVF spectrum which appeared to contain emission lines from $v > 3$. Wolfire & Königl (1991) discussed low-resolution CVF spectra obtained by Harvey *et al.* (1986) towards HH 1, and suggested that the H₂ emission is primarily excited by UV continuum fluorescence and by collisions in an UV and X-ray heated gas, rather than by collisions in a shock. And finally, Carr (1993) proposed that the weak emission towards HH 11 is caused by reforming molecules behind a fast dissociative shock. However, recent medium-resolution H₂ spectra of HH objects, obtained with IRSPEC, have cast new light on these interpretations.

2. IRSPEC Observations

IRSPEC, the ESO near-infrared spectrograph on the ESO 3.5-m New Technology Telescope (NTT), is an ideal instrument to obtain accurate spectroscopy in the 1–5 μ m range. IRSPEC provides long-slit capabilities and a spectral res-



Figures 1a, b: H- and K-band spectra of HH 43. Monochromatic fluxes F_λ in units of $10^{-13} \text{ W m}^{-2} \mu\text{m}^{-1}$ are plotted vs. wavelength λ (in μm).

olution of $R = \lambda/\Delta\lambda$ of a few 1000. The observations are reduced in a straightforward manner, using the IRSPEC context in MIDAS, which is now becoming available on-line. A graphical user interface is presently being installed at the NTT. It was developed on La Silla, with the aim to aid on-line data reduction within MIDAS, and will be described in a forthcoming article.

The high quality of near-infrared spectra that are obtained with IRSPEC is demonstrated in Figures 1a and 1b, which contain the H- and K-band emission towards HH 43. The spectra were constructed from about 20 individual grating settings, with 5–10 minutes of integration time each, equally shared between the object and the sky. It turns out that all the detected H_2 emission lines arise from vibrational levels $v \leq 3$, a strong indication that only collisional excitations occur. Upper limits for the fluxes

of lines from $v > 3$ are $F \leq 5 \times 10^{-18} \text{ W m}^{-2}$. This is in contrast with the calculations of Schwartz *et al.* (1987) who predicted line fluxes around $F \approx 10^{-16} \text{ W m}^{-2}$ for a number of lines arising from $v > 3$, such as the (6,4) Q(5) line near $1.643 \mu\text{m}$. The authors presented a CVF spectrum towards HH 43 as well, which contained a feature near the latter line, with a flux of $F \approx 10^{-16} \text{ W m}^{-2}$. From the recent IRSPEC spectrum, shown in Figure 1b, this feature is unambiguously assigned to arise from the $a^4D_{7/2} - a^6F_{9/2}$ transition of [Fe II], at a wavelength near $1.644 \mu\text{m}$.

The measured line intensities can be used to infer the population distribution among the various vibrational levels. It is conveniently examined in excitation diagrams such as those shown in Figures 2 and 3. In such diagrams, the data points can be fitted by a linear regression if, and only if, the population distribution is

relaxed to a uniform excitation temperature. This is indeed the case for HH 43, with a corresponding excitation temperature of 2200 K, represented by the full line. The dashed line is a fit to the four lowest data points and corresponds to 1900 K. H- and K-band spectra were also obtained towards a number of other HH objects. Emphasis was put to accurately measure the $1.60\text{--}1.65 \mu\text{m}$ wavelength interval, because this region is expected to show detectable emission from a number of high-excitation lines, if H_2 is non-thermally excited. None of the obtained spectra shows such lines, with upper flux limits similar to values given above. Instead, all emission arises from $v \leq 3$; the inferred population distribution is thermal in all cases and can be described by single excitation temperatures. This is demonstrated in Figure 3, where values of 2600 K, 2400 K, 2100 K, and 2100 K, respectively, were inferred for HH 54E, K, HH 56, HH 99A, and HH 106.

3. Discussion

What is the nature of the shocks that lead to the observed near-infrared emission? Since the first observation of molecular hydrogen emission in dense molecular clouds, there is considerable controversy about this question. There are two classes of shocks, which require largely different physical conditions to form. C-type (Continuous) shocks were favoured until recently, because they form under conditions that were thought typical for dense molecular clouds – low fractional ionization $x_e \approx 10^{-8}\text{--}10^{-7}$, and relatively strong magnetic fields. The fractional ionization x_e is the ratio of the electron density and the neutral gas density. J-type (Jump) shocks, on the other hand, require $x_e \geq 10^{-5}$, and can only form if the magnetic field is weak.

Near-infrared observations, together with theoretical calculations, can be used to distinguish between the two types. First, the inferred H_2 excitation temperatures are all very similar, and a single temperature is enough to fit the data for a given object. This finding points to an excitation mechanism which is insensitive to the physical conditions that prevail in the shocked regions. Such is expected for J-shocks. C-shocks, on the other hand, produce an H_2 excitation that is strongly dependent on the pre-shock density, the magnetic field strength, and other physical parameters. The observed column densities of shocked H_2 are also well modelled by slow J-shocks. C-shocks with velocities above 20 km s^{-1} produce H_2 column densities that are 2–4 orders of magnitude higher. Lower columns are produced in slower C-shocks, but then the shocks cannot raise the temperature above 1000 K,

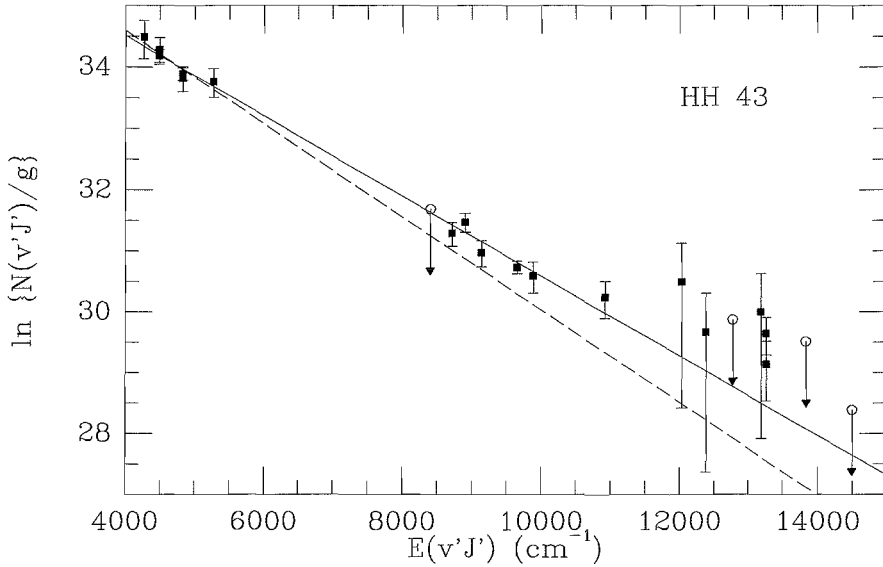


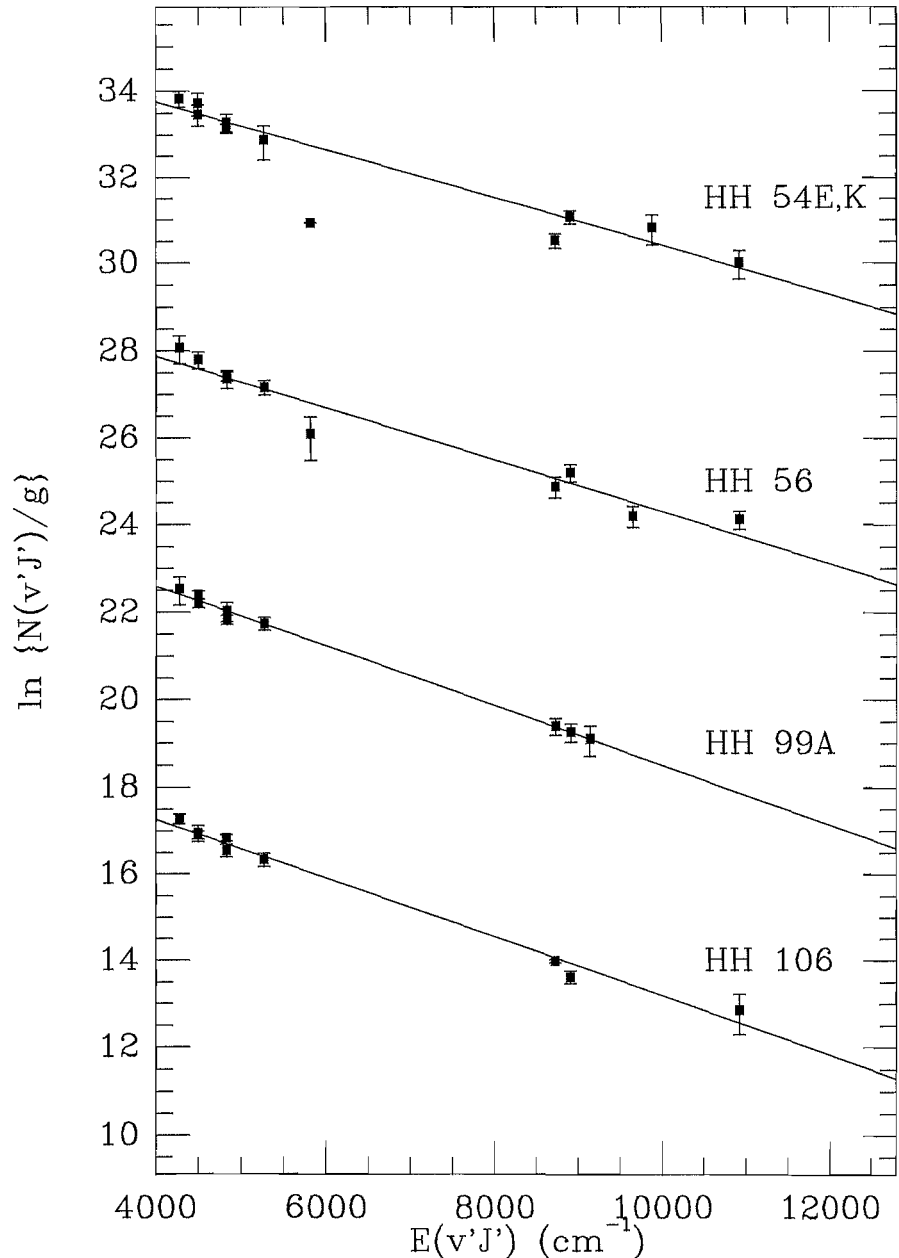
Figure 2: H_2 excitation diagram for HH 43. The full line characterizes a thermal distribution of 2200 K. The dashed line is a fit to the population density in the four lowest levels and corresponds to a temperature of 1900 K.

which is in contrast with the observations. In addition, C-shocks do not produce emission from ionized species such as [Fe II], which is present in all objects observed here. The observed [Fe II] intensities, typically a few 10^{-5} erg s^{-1} cm^{-2} sr^{-1} , agree well with the predictions of J-shock models. Last but not least, the [Fe II] observations afford the possibility to determine electron densities in the shocked region. The electron densities can then be compared with lower limits in the neutral gas density, which can be estimated from diagrams such as those shown in Figures 2 and 3. The resulting fractional ionization is high enough to mediate J-shocks.

4. Conclusions

The main result of this study is that the H_2 emission in the observed HH-objects is thermally excited by shocks. The shocks are most probably J-type, which then indicates weak magnetic fields and high fractional ionization, $x_e \geq 10^{-5}$, in the surrounding molecular clouds. Such high values of x_e may indicate that the molecular clouds have a highly clumpy, or fractal, structure. This would allow the ultraviolet photons from nearby stars to permeate deeply into the molecular material, ionize the surfaces of the clumps, and thus provide the required fractional ionization levels.

Figure 3: H_2 excitation diagrams for HH 54E,K, HH 56, HH 99A, and HH 106, with corresponding thermal population distributions of 2600 K, 2400 K, 2100 K, and 2100 K, respectively, indicated by the full lines.



It has been demonstrated that low-resolution CVF spectra are not adequate to properly interpret the near-infrared spectra of HH objects, but that indeed a resolution such as the one provided by IRSPEC is required. The need is evident to perform similar studies towards other HH objects for which non-thermal excitation has been claimed, and in particular towards those where such claims are based on low-resolution spectra. Such work is in progress.

References

- Carr, J.S. 1993, *ApJ* **406**, 553.
 Schwartz, R.D., Cohen, M., Williams, P.M. 1987, *ApJ* **322**, 403.
 Wolfire, M.G., Königl, A. 1991, *ApJ* **383**, 205.